

Joining the SAVANT Campaign: Exploring Stable Boundary Layers

AOS 404: Meteorological Measurements

Libby Carso, Andrew Kieckhefer, Leo Mikula, Vijit Maithel, Jacob Pozezinski, Claire Rubbelke, Monica Samsin, Madankui Tao, Julia Shates

1. Abstract

During the Fall of 2018, the Measurements class in the Atmospheric and Oceanic Sciences (AOS) department from the University of Wisconsin - Madison joined the SAVANT (Stable Atmospheric Variability AND Transport) team in Mohamet, IL to observe the ongoing field experiments and conduct their own measurements. Over the four day trip, students were able to observe and measure data relating to fine particle distribution, solar energy balance and general atmospheric characteristics using a variety of instruments ranging from windsonds, to dusttracks, to CO₂ gas scouters and setting up their own weather stations. This data allowed the students to explore properties of the atmosphere in a stable, nocturnal boundary layer and how the boundary layer slowly evolved and eroded following sunrise.

2. Introduction

2.1. Literature Review

In general, we are keeping these questions in mind while developing this proposal and the background to our research questions: How we can supplement the SAVANT field campaign with our work? And how are our research questions distinct? As we continue working on the project, we are working together to compile a growing list of sources to develop our understanding of boundary layer stability, radiation, particle dispersal and ecosystem response.

While the SAVANT campaign explores converging flows in the stable nocturnal boundary layer, our proposal supplements the study by expanding the scope of the work to include the sunrise transition. By also investigating the carbon dioxide (CO₂) fluxes, we will provide insight into how the ecosystem responds to cold pooling in shallow topography.

The characteristics of the stable boundary layer in Champaign-Urbana, Illinois have interested scientists for many years because of the relatively flat surface. In the late 1990s, there was a field campaign (Flatland96 Experiment) which had a wide variety of instruments over the agricultural terrain and through plots of soy and maize measuring surface fluxes, radar reflectivity and winds using sonic anemometers. The experiment also had 2m towers for temperature and humidity sensors. Avengine et al (2001) also analyze the growth of the CBL at a station in the Netherlands (Cabauw, station KNMI) with similar terrain, measurements and a 200m instrumented tower to study the boundary layer. There they examined the standard deviation of temperature, wind speed and direction in combination with profiler reflectivity to determine the onset of the CBL.

Beare (2008) use a large-eddy simulation (LES) modeling study to define the morning transition of the boundary layer. This work focuses on the role of shear in the SBL for the transition between the stable boundary layer (SBL) and the CBL. For this work, they define the transition between the SBL and CBL to occur when the sensible heat flux changes sign (from negative during the night to positive). By using the LES, they are able to determine the

sensitivity to shear during the morning transition by testing different geostrophic wind scenarios. They find that the transition is dominated by shear and the CBL, in contrast, was primarily buoyancy driven.

By exploring the stability, shear and radiative and turbulent fluxes during the SAVANT field campaign, we hope to be able to also comment on the role of shallow topography in the dissipation of the stable boundary layer. There is a connection between air pollution and dispersal of particles because the timing of the transition between the nocturnal layer and convective boundary layer (CBL) occurs during peak emissions during morning rush hour (Angevine et al, 2001). Understanding how shallow topography influences the transition may be relevant for populated areas that are situated on topography.

Mahrt, et al. 2001 and Soler, et al. 2002 both focus on the analysis of a weak gully flow that formed over the same shallow gully during CASES99. The gully consisted of a small valley with a gradient of 5%. 2D sonic anemometers and thermistors were placed across the gully to capture this flow. It was observed that a weak, thin flow occurred in the early evening on nights that had clear skies, minimum winds, and maximum temperature stratification. This flow lasted until the middle of the night, when turbulence-driven mixing and wind intensification disrupted the stratification. After midnight, a period of warming was observed, which the authors associated with downward momentum transport and minimal gully flow. In the early morning, decreases in downward mixing and turbulence prompted near-surface temperature decreases and gully flow was reestablished as the air re-stabilized. At the gully bottom, the temperature reached its minimum for the night right after sunrise.

A secondary experiment was implemented to visualize transient and special variability. Smoke releases were tracked in an effort to illustrate how “transient mesoscale motions lead to significant meandering”. Mahrt, et al. continued with data analysis and calculation of surface heat flux and characterization of the surface energy budget. Soler et al. explore the calculations regarding turbulence events that compromised the gully flow.

Pypker et al. 2007 investigated the potential for using nocturnal cold air drainage flow to monitor ecological processes. This investigation took place in a forested valley/watershed. Two aspects were explored: carbon isotope composition of the nocturnal ecosystem respiration (for the purposes of our experiment, we won't examine their methodology) and estimates of the CO₂ flux in the watershed that is advected in the drainage flow. Observation towers were assembled and deployed with thermistors, mechanical and sonic anemometers, and radiometers. A definition of cold air drainage was established, with flow needing to meet three criteria: (1) wind direction must be down valley, (2) wind-speed must have a local maximum near the ground, and (3) the net radiation measured above the tower must be negative, indicating the nocturnal surface cooling.

Results of the field measurements showed that CO₂ concentrations varied vertically with height, as well as with time. Concentrations during the day reached their highest concentration near the ground. As the air began mixing throughout the night, CO₂ concentrations from all heights converged (at this time the potential temperature profile became nearly isothermal). Following this mixing episode, concentrations rise steadily until sunrise, when drainage

remained well mixed, but concentrations began to decline. When the air again became stable, the vertical gradient of CO₂ concentration was re-established.

Basic calculations were made to provide an estimate of respiration that occurred within the watershed. Final calculated values of flux showed a range from 0.3 to 1.3 mol/s between 20:00 and 05:00. The authors discussed error sources for their calculations, as their flux values seemed low, ultimately suggesting that the remainder of the respired CO₂ may have been advected above or out of range of the measurement towers.

The concentration of PM_{2.5} is affected by solar-driven boundary layer growth and decay: while short-lifetime gases reach minima at sunrise and maxima in the evening, fine particulate matter does not show a large diurnal variation in previous studies (Tanner et al., 2005).

2.2. Hypothesis/Questions

2.2.a. Weather Station

Are weather conditions different inside and outside the gully, and how does gully flow affect these conditions?

2.2.b. CO₂ Tracker

Gully flow will occur if conditions are ideal. However, flow will be thin and easily affected by external disturbances but can be observed through a rapid shift in CO₂ concentrations. Due to stratification, flow would decrease CO₂ flux to the boundary layer due to stratification.

2.2.c. Windsond

The goal of the Windsond Team was to observe how the stable boundary layer in the atmosphere eroded during sunrise. Their observations would be obtained through a series of instrument launches throughout the morning. With each launch, the windsond instrument takes measures of air temperature, moisture and wind direction. We hypothesize that there will be a distinct shift in the temperature profile. Changes in wind speed and direction may be good indicators of a changing boundary layer. We expect the boundary layer to be heavily stratified at night and more unstable during the day. Cloudy conditions will delay the boundary layer destabilization. Clear conditions will provide the optimal observations as the sun will be able to directly warm the surface and we will be able to monitor resulting changes throughout the layer in real time.

2.2.d. Surface Energy Balance

We hypothesize that the surface energy balance at sunrise (or shortly after) will have a clear shift during the transition between a stable and unstable boundary layer. Additionally, we hypothesize there will be an indication of gully flow in the SEB.

2.2.e. DustTrak

With the change in boundary layer conditions before and after sunrise, we are curious about how it will influence the concentration of particulate matter present during the transitional

periods. We hypothesized that PM_{2.5} concentration would increase after the sunrise at a higher rate inside the valley versus outside because of the outside surface heats up faster.

3. Methods

3.1. Weather Stations

Two HOBO weather stations, Station B and Station E, were setup at locations outside and inside the gully respectively (Figure 3.4.1). There is a height difference of 13.5m between the two locations, with Station B being at the higher elevation. Each weather station was equipped with a cup anemometer, a wind vane, a temperature and humidity sensor, a pressure sensor, a solar radiation sensor, and a data logger with battery. Temperature, relative humidity, wind speed and direction, incoming solar radiation, pressure, gust speed, and dew point temperatures are recorded by the weather stations at a one-minute resolution from 14 October afternoon to 17 October morning. The data was analysed with the help of HOBOWare software and helped compare the weather conditions inside and outside the gully.

3.2. CO₂

A handheld CO₂ probe and a gas scouter were used to measure CO₂ concentrations. On one night, October 15, the handheld CO₂ probe was attached to a weather station at the base of the gully. Measurements were recorded for two time periods and analyzed to determine if CO₂ was advected through the gully to ultimately pool in the base of the gully. On October 16, the gas scouter was taken through to gully to collect concentrations during three time periods, each starting at 12 AM, 1 AM, and 2 AM local time. By taking CO₂ measurements throughout the gully at various times through the night, we were able to observe the advection of CO₂ and the evolution of air flow as the night progressed

3.3. Windsound

There were a number of processes that needed to be completed each launch to ensure that we were able to collect accurate data that would help us determine if the boundary layer destabilizes after sunrise. On launch mornings, the team would arrive at the field site no later than 6:15 A.M. This would ensure that we were able to set up the launching station and correctly link all necessary software on the computer with the windsounds. When we arrived at the field, the group set up our table and all the necessary equipment. This would include, the windsound instruments, the field computer and the helium canisters. We would then log into the computer and initiate the windsound software. All data would be collected through this program. The windsound would then be activated to establish a radio and GPS link between the computer and the instrument. It was imperative that this link is established as it is the sole pathway for collected data to be sent to the computer. Once this connection was established, a small scale weather balloon was filled with helium and tied to the windsound. A cut-off level of 400 m above the surface was established in order to get an accurate profile of the boundary layer. An electrical current would be sent through a cable in the windsound in order to cut the string attached to the balloon so that the sonde would fall back to the surface. When all steps had been completed, we would launch the balloon and watch real-time data be sent back to the computer. The windsound

would take approximately 10 minutes to reach the desired cut-off height. A GPS coordinate would be sent to the computer when the windsound had reached the ground. The retrieval team would then travel to the location to find the instrument.

3.4. Surface Energy Balance

To begin to assess the SEB at sunrise and to further explore the stability of the atmosphere, we use radiative and turbulent fluxes measured by radiometers from SAVANT NCAR observation towers. Specifically, we calculate the SEB with net longwave (**LW**), net shortwave (**SW**) broadband fluxes for the Net Radiation (**Rn**), and latent (**LH**), sensible (**H**), soil (**G**) heat flux, and assume the existence of a residual and error.

$$Rn = SW(in-out) + LW(in-out) = H + LH - G + Residual \text{ (& Error)}$$

$$LH = \underline{w'h2o'} * Lv \quad Lv = \text{latent heat of vaporization}$$

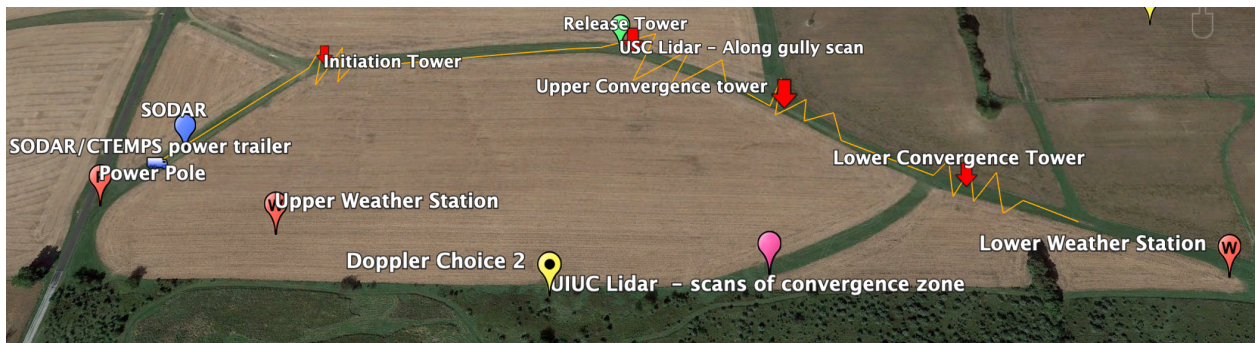


Figure 3.4.1: Schematic showing the placement of various instruments at the field site

$$H = \underline{w'T'} * \rho * Cp \quad \rho = P/(Rd*Tv) ; Cp = \text{specific heat at constant pressure}$$

The data we use are pre-quality controlled and were provided by Steve Oncley at the Earth Observation Laboratory (EOL) and is 5-minute time resolution. We apply a 30-minute running mean to the data, which smooths the terms and helps resolve turbulent eddies that develop over longer time scales (≥ 30 minutes).

For latent heat flux (**LH**), we use the covariance (2nd moment) of the anomalies of vertical motion (w') and water vapor ($h20'$). For sensible heat flux (**H**), we use the covariance for of the anomalies of vertical motion (w') and temperature (T'). For the soil heat flux (**G**), we changed the sign in the surface energy balance equation from Bonan (2008) to keep this variable consistent with the direction of the other variables in the equation.

We use observations made from the release tower and the lower convergence zone (B) at 20m height. The LW fluxes were measured by thermopiles; we calculate the density of air(ρ)using the pressure observations and the virtual temperatures calculated from sonic anemometers. The soil heat flux values are measured with a soil heat plate 5 cm below surface.

To identify the impact of shallow topography on the flow of heat/energy, we calculate the residual from the SEB equation. Then, we compare the residual values through time at the release tower and the convergence zone.

3.5. DustTrak

After the weather stations are setup and operating, begin DustTrak assembly. The two devices will be secured to the weather stations; therefore, weather stations must be set up before DustTraks. Begin with preparing the waterproof casings First, confirm that battery level is at 99% or higher before starting. Screw the PM_{2.5} filter onto the intake hole. Program DustTrak with desired DustTrak parameters. In this case, collecting PM_{2.5} concentrations every second.

To prepare the waterproof casing, puncture a hole the side of 1m tubes. Hole should be just larger than the diameter of the 1m tubing. Secure one end of the 1m tubing 1.5 meters above the ground. The tube should open to the sky and the rest should feed below 1.5 meters. Feed the other ends of the tubes into cases about 1/3 the length. This will make the next step easier. Insert the end of PM_{2.5} filter into the end of the tube inside the casing. Once snug, pull out any tube excess so the DustTraks can rest comfortably in the cases after inserted. Place the cap on waterproof cases and close on all sides.

Once the DustTraks are inside the secured cases, we configured two Zip Ties to each side of the containers and tied them around the weather stations' legs. While this is going on, we hear the DustTraks buzz, meaning they are working properly. Now we wait for our data to collect. In the meantime, we supported and observed other portions of the field experiments. Let DustTraks collect data for 3 hours. Overall, 6 sets of data should be collected, each with 3-hour intervals of PM_{2.5} concentration readings. Devices should be started 1.5 hours before sunrise and then turned off 1.5 hours after sunrise. After data collection and retrieval, we need to have the field data logged on the field laptop. Connect the two devices and upload the data then save. Make sure DustTraks have enough battery life to support another morning of data collection.

4. Results

4.1. Weather Stations

Different weather conditions were observed during the three nights of experimentation. The night of 14th October was rainy along with high winds associated with a cold front passing through the area. Night of 15th October was clear with very low winds, making it ideal for gully flow. An IOP was conducted by the SAVANT team on this night. Night of 16th October, although clear, had relatively higher wind speeds. Data from the two weather stations is shown in the following figures, with data from Station B

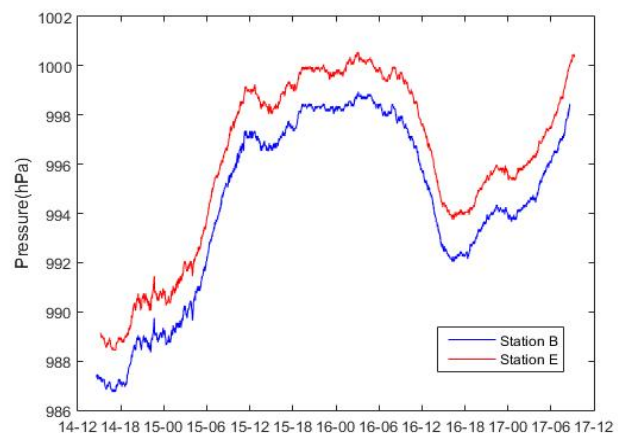


Figure 4.1.1: Pressure measured in hPa at Station B (blue) and station E (red).

(outside the gully) in blue and data from Station E (inside the gully) in red.

From hydrostatic balance, a pressure difference of around 1.6hPa is expected between the two locations due to the 13.5m difference in heights, with pressure being higher at lower location (Station E). This is observed in figure 4.1.1.

The wind vane is setup such that values closer to 0° (or 360°) represent winds coming from the north, 90° represents winds from the east, 180° represents winds from south, and 270° represents winds coming from the west. Figure 4.1.2 shows wind speed (top) and direction (bottom). Strong winds are coming from a north, north-west direction on 14th night and 15th morning, which can be expected during passage of a cold front. Wind flows from a western direction in general for the rest of the days. Winds

were considerably calmer on the night of 15th October. Also, winds inside the gully (Station E) at Station B (blue) and station E (red) are clearly weaker compared to winds outside the gully.

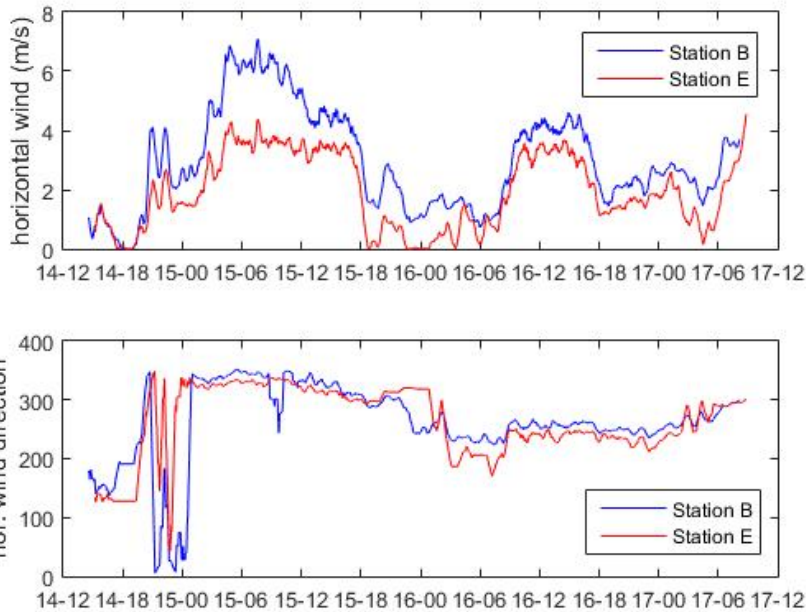


Figure 4.1.2: Wind speed (top panel) and wind direction (bottom panel) at the two weather stations

Figure 4.1.3 shows the temperature measured at the two weather stations. Diurnal cycle is clearly visible in the time series. Temperature measured at the lower convergence tower is also plotted in black to compare with another location inside the gully. Overlap of red and black curves, show that temperature is fairly uniform along the gully at all times. Furthermore, the temperature is almost the same inside and outside the gully for most times during the observation period, with the exception on the night of 15th October, when temperatures inside the gully are cooler compared to outside.

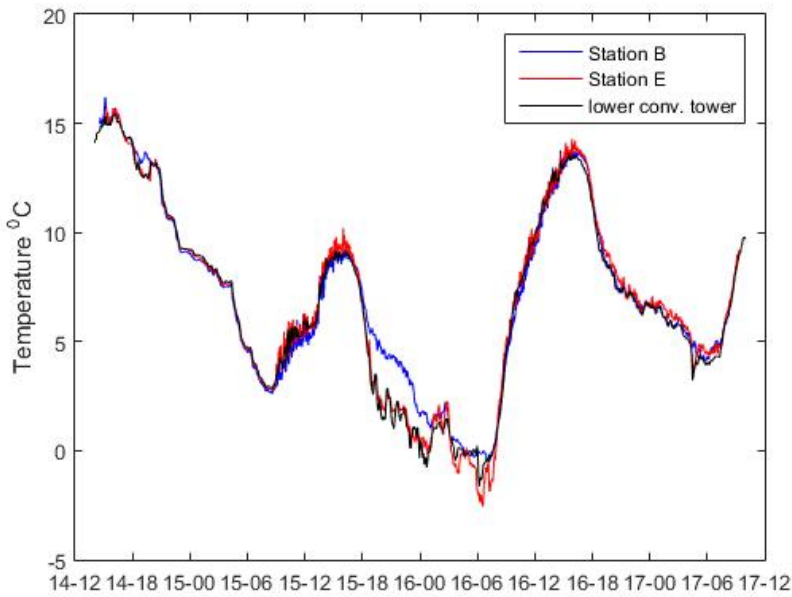


Figure 4.1.3: Temperature at different locations. Station B (blue), Station E (red), and lower convergence tower (black)

4.2. CO₂

The conditions at midnight on October 15 were 48°C with occasional gust speeds of 3.94 mph from the north and northwest; there were precipitation and overcast clouds. The conditions at midnight on October 16 were 32.9°C with little-to-no winds from the west and northwest; there were no precipitation or extensive cloud cover. On October 17, the temperature was 44°C with a wind speed of 5 mph from the southwest direction.

Data from the gas probe varied little through the period of collection. The peak value was 391 ppm, and the low was 383 ppm. Overall, the concentration remained fairly constant through the time of observation.

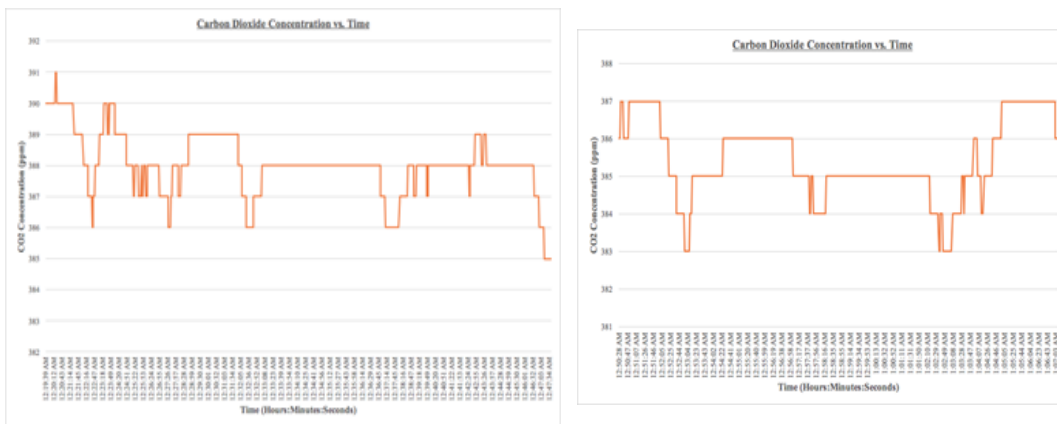


Figure 4.2.1: Carbon di-oxide concentration measured from probe inside the gully on 15th October.

Data from the gas scouter during all three runs showed lower concentrations of around 430 to 470 ppm at the top of the gully, with an increasing trend of concentrations toward the base of the gully. The highest concentration was 1052 ppm. Higher concentrations occurred later in the evening.

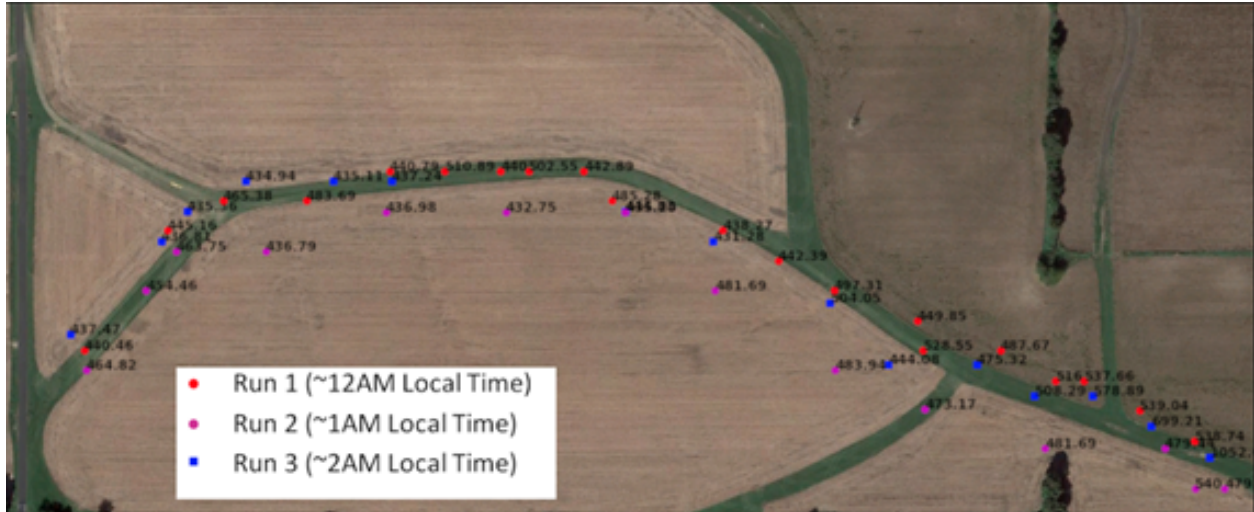


Figure 4.2.2: Image showing spatial map of carbon dioxide concentration as measured during the three gas scouter runs

4.3. Windsond

The best data from the three days of measurements came from October 17th. This day provided the group with clear conditions and calm winds. We were able to launch the windsonds every 30 minutes and had no issues with any of those launches. The data we received from the instruments showed the slow destabilization of the boundary layer throughout the morning.

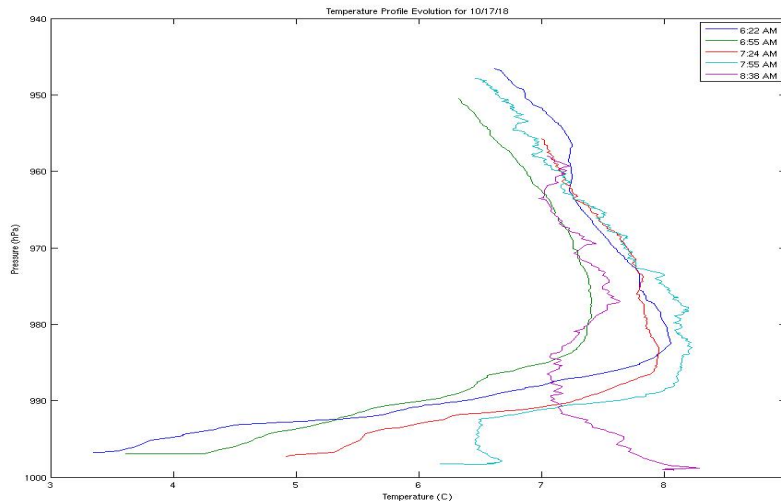


Figure 4.3.1: The temperature profile of the atmosphere during the sunrise transition is shown. Each colored plot corresponds to a morning launch (occurring every 30 minutes). Note the gradual warming near the surface, emphasizing an evolving boundary layer.

The figure above shows the temperature profile throughout the morning of October 17th. Each line is color coded to correspond to launch times of the windsonds. The early morning launches all occurred before sunrise (7:04 AM on this day). As shown, the temperature profile at the 6:22 AM and 6:55 AM launch illustrates a stable boundary layer just above the surface. Once the sun began heating the surface and mixing near the surface occurred, the temperature near the surface began to increase. The temperature profile from the last morning launch, happening at 8:36 AM, shows a more unstable layer near the surface as compared to the first windsond launch at 6:22 AM on the 17th. The lapse rate is measured to be near the dry adiabatic lapse rate (9.8 degrees C/Km).

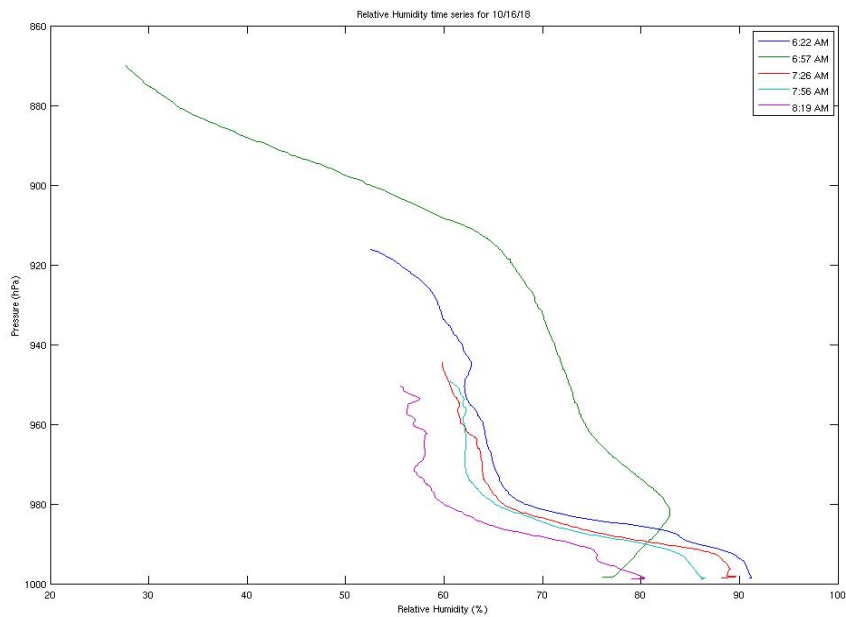


Figure 4.3.2: Plot of the measure atmospheric relative humidity before, during and after sunrise on October 16th. Different launch times are shown in varying colors.

There were a number of other interesting results from the data that was collected by the windsonds. During sunrise, the relative humidity observed slowly decreased once the sun rose. This is not a surprising result as the temperature increased while the dew point remained constant. The wind speed just above the surface (100-200 meters) gradually increased as well. This resulted in higher atmospheric shear at lower levels, enhancing mixing near the surface.

4.4. Surface Energy Balance

For the results of the SEB analysis, we focus on Monday/Tuesday 15-16 October, which was one of the nights that the SAVANT researchers forecasted conditions favorable for a stable, nocturnal boundary layer. In the figures below, we can identify a shift in all of the radiative and turbulent fluxes at sunrise (~7:05am). Net radiation switches sign to positive with increasing shortwave radiation from the sun- the surface is no longer radiatively cooling. It is apparent that there is a time lag from when Rnet switches sign and when the turbulent fluxes and soil heat flux respond and switch sign. With the exception of the soil heat flux G, H takes the longest time to respond to the incoming shortwave radiation. In contrast to the fluxes, the SEB residual appears to lead (or aligns very closely with) the Rnet when it begins to increase.

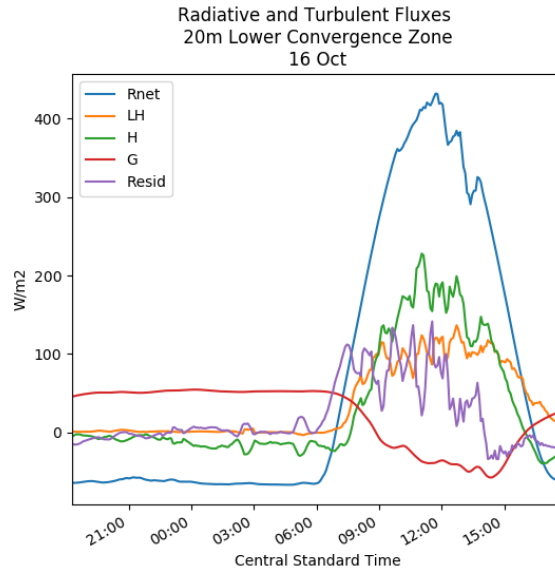
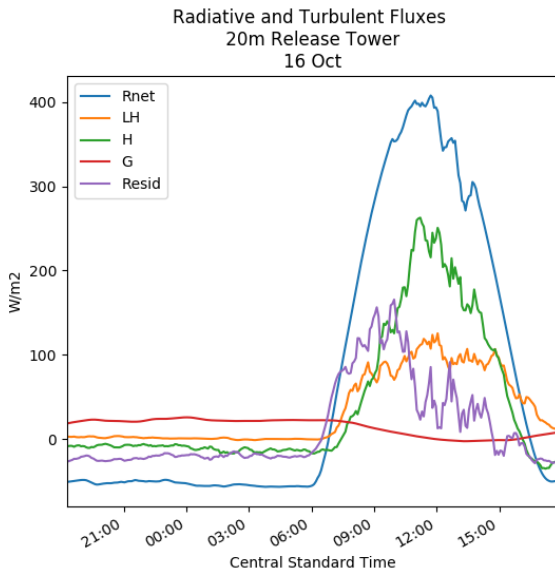
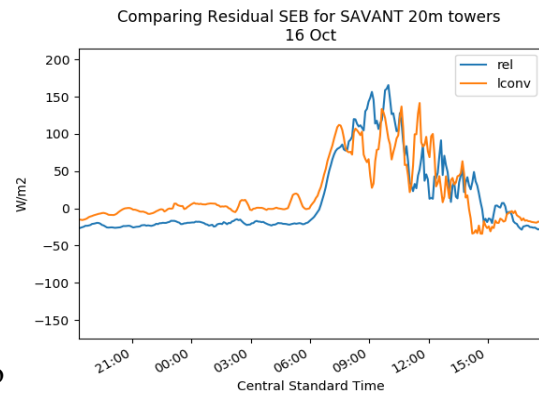


Figure 4.4.1a (above): Time series of radiative and turbulent fluxes starting in the evening (15 Oct) and ending in the afternoon (16 Oct). Sunrise in Mahomet, Illinois: 7:05am (CDT)
 Figure 4.4.1b (right): Time series of residual from SEB starting in the evening (15 Oct) and ending in the afternoon (16 Oct)



The calculated SEB residuals stay close to zero throughout the night at the release tower and the lower convergence zone. During the nighttime hours, however, the lower convergence appears to have more blips in the time series. The two residuals have a correlation of 0.8. For the lagged correlation at 5 minutes, the value decreases to 0.79 and continues to decrease to 0.76 at 20 minutes.

4.5. DustTrak

We have first compared the $PM_{2.5}$ concentrations between two weather stations. We hypothesized that the concentration for $PM_{2.5}$ is higher outside of the gully since it heats up more quickly. Through a T-test between the two stations, we found strong support to our hypothesis with P-value smaller than 0.01, which indicates that the concentration of fine particulate matter is higher on the Upper Tower outside of the valley. Then we did a similar test by dividing data to before and after sunrise. Due to an increase in temperature and disturbance in the stable boundary layer after sunrise, we hypothesized that $PM_{2.5}$ concentration would also increase. The statistical test gives a p-value smaller than 0.01 and provides strong support to our hypothesis. In sum, we found that $PM_{2.5}$ concentration would increase after the sunrise at a higher rate inside the valley versus outside.

Besides comparing $PM_{2.5}$ for different locations and period, we try to associate it with meteorological variables measured by the weather stations. Through Pearson correlation analysis, we found that temperature is positively related to $PM_{2.5}$ concentration (with Pearson correlation coefficient of 0.57) while relative humidity is negatively associated with $PM_{2.5}$ concentration (with Pearson correlation coefficient of -0.62). Solar radiation and wind speed and direction do not show a linear relationship with $PM_{2.5}$.

Of the weather variables we compared with $PM_{2.5}$ concentrations, relative humidity and temperature were the most significant.

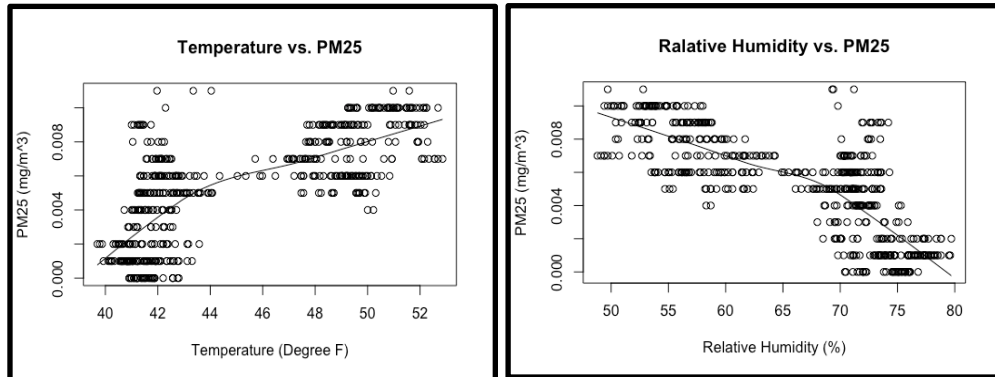


Figure 4.5.1: $PM_{2.5}$ concentration as a function of temperature (left) and relative humidity (right)

The above figure shows relationships between $PM_{2.5}$ and temperature (left) and $PM_{2.5}$ and relative humidity (right). On the left-hand side, the data indicate that an increase in air temperature is related to higher concentrations of $PM_{2.5}$. We observe the opposite situation regarding relative humidity on the right-hand side — less relative humidity in the air related to a decrease in the observed $PM_{2.5}$ concentrations. These results are consistent with what we would expect.

5. Discussion

5.1. Weather Stations

Cold air drainage flows in shallow topography are very sensitive to the local weather conditions. Clear skies, and low wind conditions are most ideal for such a flow to be established (Mahrt, et al. 2001). Such a flow of cold, high density air through the gully should be reflected in temperature measurements inside the gully. Figure 4.1.3 shows that on the night of 15th October, when there were low wind and clear sky conditions, temperature inside the gully is lower. On the other two nights, when the weather conditions did not allow for gully flow to be setup and there is no cold air flowing through the gully, no temperature difference is observed between locations inside and outside the gully.

5.2. CO_2

Data from both the probe and the gas scouter supports the idea that katabatic gully flow forms in environments where the air is densely stratified. This occurs on nights when there is low cloud cover, which allows for more radiative cooling and the formation of a nocturnal boundary

layer (Soler, et al., 2002; LeMone, et al., 2003). Observations from the gas probe showed that on a night with overcast skies, there was not enough radiative cooling to induce the stratification necessary for the formation of the boundary layer.

The gas scouter recorded thousands of concentrations, and not all could be plotted. The investigators used a formula to parse through the data and create a separate data file which contained every 150th data point. This was done to create a clear and easy to read map of the spatial distribution of CO₂ concentrations through the gully.

5.3 Windsond

There were a number of challenges that arose during our data collection that required special attention or alteration of launch times. These challenges were encountered early and we were able to accurately address the issues. On our first official launch day, Monday, October 15th, the weather proved to be anything but ideal. A thick lower cloud layer prevented any substantial heating by the sun, significantly affecting the measurements taken by the windsond. However, this was not the biggest issue we encounter due to weather. This day also was the windiest of the week, causing major issues for the single windsond we launched in the morning. As we were still learning the proper settings for each launch, the cut-off point for the sond was set at (number), much higher than the final level that was determined for the group. The strong wind, combined with a high cut-off level, allowed the windsond to travel very far from the launch location. This result encouraged the group to limit the number of launches initiated on windy days. If the wind was too strong, launches would be postponed for the day.

These issues were fairly minor and only required slight alterations in scheduling for launches and settings for each windsond. Our greatest challenge, however, was directly related to hardware of the windsondes. As previously mentioned, we were required to set a cut-off level for each windsond prior to the launch. Once the windsond passed this level in the atmosphere, an internal wire would heat up and burn the string connecting the windsond to the weather balloon. The windsond would then fall to the ground where it would be retrieved by a team of students. During one of the initial launches, this cutting mechanism failed and prevented the windsond from returning to the ground. Though we were still able to collect data, we were unable to retrieve the windsond. In the end, we were able to construct a beautiful atmospheric profile as the windsond rose far past the desired cut-off level. This specific windsond also traveled nearly 18 miles from its original location before we lost radio contact. In all, we lost a total of 4 windsondes, 2 from failed shutdown mechanisms and 2 due to inability to locate them on the ground (one falling in a dense forest and another landing in the middle of a lake).

5.4. Surface Energy Balance

The sensible heat flux (H) changing sign is an indication of the destabilization of the stable, nocturnal boundary layer (Bonan, 2008). Turbulent eddies are able to develop within the boundary layer, but the measurements show that the transition is not immediate- there is a time lag from R_{net} increasing and H increasing (and ultimately changing sign). The soil heat flux (G) switches sign from positive to negative as the ground is no longer a source of heating to the atmosphere but begins to absorb energy. The increasing LH is evidence for evaporation within

the boundary layer, and the curves for the release lower convergence towers appear coherent. This suggests that evaporation may not differ largely from the two towers, so, it appears to occur at a larger scale independent of the shallow topography.

The changes in the residual from SEB equation at both towers align very closely with the Rnet changes. This term in the equation may identify the start of the transition to a destabilized atmosphere. During the night time, the residual at the lower convergence tower is consistently higher than at the release tower. Considering the equations are very close to being balanced, and that turbulent eddies from H are close to zero, we may be able to infer gully flow from the release to the lower convergence zone. The correlation (0.8) between two locations is highest when looking at the same time step; a lag 5 - 20 minutes decrease the value, which contrasts with what I expected. It is possible that using a 5-minute running mean may remove some of the phase lag in the flow along the gully.

5.5. DustTrak

By comparing the variation of DustTrak concentrations of PM_{2.5} before and after sunset, as well as inside and outside a gully, we found that PM_{2.5} concentration is significantly higher outside the gully after sunrise. This study supported both of our hypotheses. This finding confirms our expectation that disturbance of the nocturnal stable boundary layer after the sunrise with lead to an increase in PM_{2.5} level.

We used the weather station data to justify the pattern we observed for PM_{2.5}. We find a moderate positive correlation between PM concentration and temperature and a moderate negative relationship between PM concentration and relative humidity. This is reasonable since higher temperature, and the drier atmosphere is often related to higher PM concentration and explains what we observed for the morning transition. Besides, the temperature increased after sunrise, which disturbed the stable nocturnal boundary layer formed during the night. As stratified air started to move, observing an increase in PM level at 1.5 meters was unsurprising.

We also did the same linear analysis for wind speed and direction but did not find any relationship between PM concentration and any of these two variables with a small magnitude of Pearson correlation coefficients. We expected to see a connection with at least one variable for a few reasons. Fine particulate matter may result from the wind blowing in PM_{2.5} from an area of higher concentrations. Most of the PM_{2.5} arrived from southwesterly winds. While this was a trend, it was not significant. Wind speeds had little to no relation to the PM_{2.5} content in the air.

There are certain limitations for this study that need justification for future research. Firstly, we only collected PM_{2.5} data for three days with a three-hour duration each day. More data points are necessary to confirm the pattern indicated by this study. Secondly, one of the DustTraks automatically turned off as a result of the cold temperature before sunrise. Future measurements should pay attention to the operation range of the measurement tool to avoid such failure.

6. Conclusions

6.4. Weather Stations

The data collected from the two weather conditions helped study the weather conditions inside and outside the gully. The difference in pressure at the two locations matched with the expected pressure differences due to elevation from hydrostatic balance. Wind speeds were noticeably weaker inside the gully, possibly because of a shielding effect by the shallow topography. Gully flow when setup brings cold dense air into the gully, making the gully cooler than outside regions.

6.2. CO₂

Gas scouter data highly suggests the presence of a nocturnal boundary layer, which then manifested as down-slope flow. Run 1 implies a slight drainage present, with measurements from the top and base of the gully only varying by about 100 ppm. Run 3, started at ~2AM, suggested a strengthening of flow as the night progressed. At this point the concentration of CO₂ at the top of the gully was recorded at 437ppm and increased through the gully with a final reading of 1052 ppm at the base of the gully. Presence of a cold pool (Whiteman, 2000) at the base of the gully is thus inferred.

Run 2 recorded data from a track adjacent to the gully. This yielded reading of CO₂ concentration that showed little variance as the gully was traversed. The reading at the top of the gully was 432.74 ppm and the average CO₂ concentration at the base of the gully was 480 ppm. This data shows that a weak general flow may have formed outside of the gully, but more evidence would be needed to verify this claim.

The third hypothesis was unable to be tested because of time and money restrictions.

6.3. Windspeed

The group hypothesized that there would be a noticeable shift in the temperature profile of the atmosphere during the transition for a stable to unstable boundary layer during sunrise. After conducting numerous launches during our three-day collection period, the data received supports this hypothesis as there was a distinct change in the temperature near the surface throughout sunrise. The temperature gradually rose, causing the boundary layer to become more unstable after sunrise. Changes in wind speed and relative humidity also illustrate the atmospheric transition to a more unstable boundary layer.

6.4. Surface Energy Balance

To better understand the transition from stable to convective boundary layer, it is important to assess the changes in radiative and turbulent fluxes for more than one night/morning. While the night & morning of 15-16 October was ideal for exploring the research questions, without other cases, it is uncertain whether the characteristics of the Surface Energy Balance in this paper represent most transitions or if the results were anomalous. Realistically, this is a reasonable task that can be pursued. There are two different approaches to studying the transition in the future with the NCAR/EOL tower data: 1) analyze all days that were flagged as having a stable nocturnal boundary layer to characterize the transition or 2) use criteria from the 16 Oct. case to identify these days and compare to the days flagged by SAVANT researchers.

In addition to more data, this section of the work can also be expanded by exploring the SEB terms through more statistical methods such as using the cross-correlation function to understand the lead/lag and relationships. In addition, significance testing is needed for correlation values.

6.5. *DustTrak*

Our group hypothesized that PM_{2.5} concentration increases after the sunrise and is higher outside of the gully during this period. Based on data collected before and after sunrise, both hypotheses were supported with statistical significance. During the morning transition period, level rises as the nocturnal boundary layer are disturbed by the heating of the land surface, and this heating process happens at a faster rate outside of the gully. We also found moderate associations between PM_{2.5} with temperature and relative humidity. No direct association with wind speed and wind direction was found in this study.

7. References

- Angevine WM, Baltink HK, Bosveld FC (2001) Observations of the morning transition of the convective boundary layer. *Boundary-Layer Meteorol* 101:209–227
<https://link.springer.com/content/pdf/10.1023%2FA%3A1019264716195.pdf>
- Beare RJ (2008) The role of shear in the morning transition boundary layer. *Boundary-Layer Meteorol* 129:395–410
<https://link.springer.com/article/10.1007/s10546-008-9324-8>
- Bonan, G. (2008). Surface energy fluxes. In *Ecological Climatology: Concepts and Applications* (pp. 192-204). Cambridge: Cambridge University Press.
doi:10.1017/CBO9780511805530.014
- Mahrt, L., Vickers, D., Nakamura, R., Soler, M., Sun, J., Burns, S., & Lenschow, D. (2001). Shallow Drainage Flow. *Boundary Layer Meteorology*, 243-260. Retrieved from
<https://pdfs.semanticscholar.org/b656/48b430b65486a2af969d26e2f0c8938a8df7.pdf>.
- Pypker, T. G., Unsworth, M. H., Mix, A. C., Rugh, W., Ocheltree, T., Alstad, K., & Bond, B. J. (2007). Using Nocturnal Cold Air Drainage Flow To Monitor Ecosystem Processes In Complex Terrain. *Ecological Applications*, 17(3), 702-714. doi:10.1890/05-1906
- Soler, M., Infante, C., Buenestado, P., & Mahrt, L. (2002). Observations Of Nocturnal Drainage Flow In A Shallow Gully. *Boundary-Layer Meteorology*, 105(2), 253-273.
doi:10.1023/a:1019910622806
- Tanner, R. L., Bairai, S. T., Olszyna, K. J., Valente, M. L., & Valente, R. J. (2005). Diurnal patterns in PM_{2.5} mass and composition at a background, complex terrain site. *Atmospheric Environment*, 39(21), 3865–3875. doi: 10.1016/j.atmosenv.2005.03.014